

Article

Yeast-Based A β 1-15 Vaccine Elicits Strong Immunogenicity and Attenuates Neuropathology and Cognitive Deficits in Alzheimer's Disease Transgenic Mice

Dong-qun Liu ^{1,2}, Shuai Lu ¹, Lun Zhang ^{1,2}, Ya-ru Huang ^{1,2}, Mei Ji ^{1,2}, Xiao-ying Sun ^{1,2}, Xiao-ge Liu ^{1,2} and Rui-tian Liu ^{1,*} 

¹ National Key Laboratory of Biochemical Engineering, Institute of Process Engineering, Chinese Academy of Sciences, Beijing 100190, China; dqliu@ipe.ac.cn (D.-q.L.); slul@ipe.ac.cn (S.L.); zhanglun@ipe.ac.cn (L.Z.); yrhuaug@ipe.ac.cn (Y.-r.H.); jimei@ipe.ac.cn (M.J.); xysun@ipe.ac.cn (X.-y.S.); xgliu@ipe.ac.cn (X.-g.L.)

² School of Chemical Engineering, University of Chinese Academy of Science, Beijing 100049, China

* Correspondence: rtlui@ipe.ac.cn; Tel.: +86-10-82545017; Fax: +86-10-82545025

Received: 6 June 2020; Accepted: 29 June 2020; Published: 1 July 2020



Abstract: Immunotherapy focusing on reducing the amyloid-beta (A β) burden is a promising treatment strategy for Alzheimer's disease (AD). Many clinical studies on AD immunotherapies have failed due to low safety and efficacy, calling for a highly potent AD vaccine which induces sufficient antibody titer while avoiding side effects. Here, we designed a yeast-based vaccine Y-5A15 comprising five copies of A β 1-15 displayed on the surface of yeast cell wall, and we subcutaneously immunized APP/PS1 mice three times. Our results demonstrated that the Y-5A15 remarkably enhanced the A β epitope immunogenicity and elicited high antibody titers against A β in AD mice. Importantly, Y-5A15 vaccination successfully reduced A β levels, plaque burden and glial activation, rescued synaptic deficits and significantly ameliorated memory and cognitive decline in APP/PS1 transgenic mice, suggesting that the yeast-based A β epitope vaccine has a promising potency for the treatment of AD.

Keywords: Alzheimer's disease; beta-amyloid; active immunotherapy; yeast; vaccine

1. Introduction

The neuropathologies of Alzheimer's disease (AD) are characterized by deposition of β -amyloid (A β) peptide in senile plaques and the formation of intracellular neurofibrillary tangles (NFT) [1,2]. A β peptides have been confirmed to play a central role in the onset and progression of AD for over 20 years, and the soluble A β oligomers and protofibrils, which are now considered to be the most toxic forms of A β , responsible for synaptic destruction [3–6]. Anti-A β immunotherapy is an efficient strategy to relieve the A β burden, which has been verified in various AD transgenic models. Unfortunately, the first vaccine clinical trial in AD patients (AN-1792) failed due to meningoencephalitis in 6% of immunized AD patients, which was associated with autoreactive T cell infiltration into the brains of immunized subjects in combination with a strong, Th1-based adjuvant, QS21 [7–9]. Another major issue with the AN-1792 vaccine was insufficient antibody titer due to the weak immunogenicity of A β , which limited the therapeutic effect [10–12].

Notably, the dose-dependent effect of anti-A β oligomer/protofibril antibodies on A β burden and cognition was recently demonstrated in patients with mild AD [7,10,13]. An expanded dataset from the phase 3 EMERGE trial on patients receiving high-dose aducanumab reported statistically significant changes in the Clinical Dementia Rating-Sum of Boxes (CDR-SB) scores [14], suggesting that a potential A β -based vaccine should be administered preventatively and induce robust antibody

titer to halt or at least delay the development of AD pathologies. To avoid autoreactive T cells against A β and to generate relatively high titers of antibodies, the secondary generation of A β vaccine was developed by conjugating B-cell epitopes, N terminus of A β 42 to foreign carriers to overcome low immunogenicity of B-cell epitopes [15–18]. However, none of the above AD vaccines has produced clinically meaningful results, calling for a more optimal vaccine platform for the future development of A β epitope vaccines.

The yeast cell is a promising vaccine carrier and adjuvant which can be naturally recognized by APCs and has been approved by the US Food and Drug Administration (FDA) for clinical test, generally recognized as safe (GRAS) by FDA [19,20]. Some studies have shown that recombinant EBY100 *Saccharomyces cerevisiae* is an effective vaccine carrier, which expresses antigens on the cell wall through a yeast display system [21,22]. Yeast using a surface display system can express high-density heterologous proteins, is easily prepared, extremely stable and low cost [23,24]. Moreover, the epitopes displayed on the surface of particles can provide the most efficient antigen presentation to B cells, which is benefit for inducing rapid and robust antibody response [25]. Thus, the yeast cell is considered to be a superior vaccine development and antibody induction platform.

In order to induce sufficient antibody titer against A β and efficient improvement on cognitive capacity, we developed Y-5A15 yeast cell as a vaccine carrier and immune adjuvant, comprising five copies of A β 1-15 displayed on the yeast cell wall, and assessed its therapeutic effect on APP/PS1 mice.

2. Materials and Methods

2.1. Materials

EBY-100 *S. cerevisiae* strain was kindly provided by Dr. Xiang-mei Liu, Shandong University, Jinan, China. The A β 42 and A β 40 immunoassay kits were purchased from Immuno-Biological Laboratories Co., Ltd. (Gunma, Japan). 6E10 (monoclonal antibody against A β 1-16; BioLegend, San Diego, CA, USA), 4G8 (monoclonal antibody against A β 17-24; Signet Laboratories/Covance Research Products, Denver, PA, USA), 9E10 (anti-c-Myc antibody, Santa Cruz, CA, USA), Iba-1 polyclonal antibody (Genetex, Irvine, CA, USA), and GFAP monoclonal antibody (Cell Signaling Technology, Danvers, MA, USA). HRP-conjugated goat anti-mouse IgG antibody and FITC-conjugated goat anti-rabbit IgG antibody were obtained from Beijing Zhongshan Golden Bridge Biotechnology Co., Ltd. (Beijing, China).

2.2. Preparation of Yeast-Based Vaccine

To enhance the immunogenicity of the epitope peptides, the gene fragment encoding the five copies of A β 1-15 fragment was inserted into a modified vector of pCTCON2 and transfected into EBY-100 (*Saccharomyces cerevisiae*) using the method described previously [26]. The epitopes displayed on the yeast cells were then assayed by flow cytometry and confocal microscopy after probed with FITC-labelled anti-c-Myc antibody. The EBY100 carrying the vehicle vector was the negative control. The EBY-100 cell-based vaccine was heat-inactivated for 1 h at 56 °C and stored at –80 °C until use.

2.3. Mouse Immunization

Six-month-old APP/PS1 transgenic AD mice were obtained from Jackson Laboratories (Bar Harbor, ME, USA). The transgenic mice were randomly assigned to treatment with yeast vector control YEVC ($n = 6$), Y-5A15 ($n = 6$), or AD control ($n = 6$), and their WT littermates ($n = 6$) were used as a positive control for the behavior test. The mice were immunized 3 times with 6×10^7 cells in biweekly intervals. Blood was collected in regular intervals and stored at –80 °C until use. The effects of Y-5A15 on the cognition of AD mice were detected 20 days after the last administration. All experimental protocols were approved by the Tsinghua University Animal Care and Use Committee and were performed in accordance with the China Public Health Service Guide for the Care and Use of Laboratory Animals.

2.4. Antibody Titer Determination

The titers of vaccine-induced antibodies in mouse sera against A β 42 peptide were determined by indirect enzyme-linked immunosorbent assay (ELISA). Briefly, 96-well ELISA plates were coated with A β 42 peptide (0.5 μ g/well) at 4 °C overnight and blocked with 3% (*w/v*) bovine serum albumin in PBS for 2 h at 37 °C. After blocking, 2-fold serial dilution of sera were added in triplicates and incubated for 2 h at 37 °C. The bound serum antibodies were detected with HRP-conjugated anti-mouse IgG and TMB substrate. The reaction was stopped by adding 2 M H₂SO₄, and the absorbance of OD450 nm were read on microplate reader MD-SpectraMax M5 (Molecular Device, Sunnyvale, CA, USA).

The levels of different IgG isotypes were also assayed by ELISA with the HRP-conjugated anti-mouse -IgG1, IgG3, -IgG2a and -IgG2b antibodies as the secondary antibodies (Abcam, Cambridge, UK), respectively.

2.5. Novel Object Recognition (NOR) Test

Mice have the spontaneous tendency to exhibit more interactions with a novel rather than a familiar object. Each mouse was put in a white box at 40 × 40 × 40 cm and allowed to freely explore the open field arena without objects in the habituation phase. Each mouse was then put in the box containing two identical objects for another 5 min during the familiarization period. Recognition memory was assayed after 24 h by exposing the mouse to one familiar and one novel object. The exploring and sniffing times on each object were recorded.

2.6. Y-Maze Test

The Y-maze test was executed to assess short-term memory capacity of mice. Y-mazes consist of three arms with an angle of 120° between each of the two arms. The three identical arms were randomly designated: the start arm kept open, in which the mouse was put to start exploring, the novel arm was open just during the 2nd trial but blocked during the 1st trial, and the other arm was always kept open. To assess the spatial recognition memory, the Y-maze test had two trials separated by 1 h of inter-trial interval (ITI). The first trial (training) had a 10 min duration and allowed the mouse to explore the start arm and the other arm, with the third arm (novel arm) being blocked. After 1 h ITI, the mice were placed back to the maze in the same starting arm, with free access to all three arms for 5 min during the second trial. All trials were recorded on a videocassette recorder using a ceiling-mounted charge-coupled device (CCD) camera, and the number of entries and time spent in each arm in the video recordings were analyzed.

2.7. Morris Water Maze (MWM) Test

The MWM test was performed in a 1.2-m-diameter white iron pool at 22 ± 1 °C during 5 training days. The mice were released into the pool at one designated start location for each trial and were allowed to find a platform hidden 1–2 cm under the water surface. Each training lasted 60 s until to find hidden platform. All the mice were allowed to stay on the platform for 10 s. The swimming activity of each mouse was recorded by an automated overhead-mounted video tracking system (Sony Corp., Tokyo, Japan). On day 6, the platform was removed from the pool and the mouse were allowed to explore the pool for 60 s, and then the escape latencies, the time in the target quadrant and the number of target crossings were measured.

2.8. Cerebral Homogenate Collection

After the behavioral tests, all mice were deeply anesthetized and perfused with ice-cold PBS containing 10 U/mL heparin. Half brains were dissected and rapidly homogenized. The brain tissues were bounce homogenized in solubilization buffer containing protease inhibitor cocktail (50 mM Tris, pH 7.4, 150 mM NaCl, 2 mM EDTA, 1% sodium deoxycholate, 1% Triton X-100), then centrifuged at

14,000× *g* for 30 min at 4 °C. The supernatant was used to assess soluble A β . The insoluble pellets were homogenized with 2% SDS buffer (50 mM Tris, pH 7.6), and centrifuged at 14,000× *g* for 1 h at 4 °C to obtain supernatants containing insoluble A β .

2.9. Measurement of A β 40/42

To detect soluble and insoluble A β levels in the brains, an anti-human A β ₁₋₄₂ and A β ₁₋₄₀ ELISA kits were used according to the manufacturer's instructions. The levels of soluble and insoluble A β were standardized to the brain tissue weight.

2.10. Immunohistochemistry (IHC)

Immunohistochemical staining was performed as previously described [27]. Briefly, brain cryosections (20- μ m thick) were treated with 80% (*v/v*) methanol containing 0.3% H₂O₂ to prevent endogenous peroxidation. After blocking with 10% goat serum, the sections were incubated with primary antibodies 4G8 (1:100), 6E10 (1:100), Iba-1 (1:100) or GFAP (1:100) for 1 h at room temperature (RT), and then incubated with a fluorescent-labeled secondary antibody at RT for 30 min. Images were collected on an Olympus BX60 microscope (Olympus Optical Co., Ltd., Tokyo, Japan) or confocal scanning laser microscope (LSM780, Zeiss, Oberkochen, Germany), respectively. For analysis of the images, we used IpWin5 analysis software.

2.11. Statistical Analysis

The data were expressed as mean \pm SD. The data was processed and analyzed with GraphPad Prism 6.01. ELISAs data were performed at least three times for each experiment, and six mice per group were analyzed for behavior tests and IHC analysis. Data were analyzed using one-way ANOVA or Student's *t*-test. Differences were considered significant at * *p* < 0.05, ** *p* < 0.01, and *** *p* < 0.001.

3. Results

3.1. The Preparation of Y-5A15 Vaccine

To induce maximal antibody titer and avoid the activation of autoreactive T-cells, we used five copies of A β ₁₋₁₅ as the antigen and the EBY100 *Saccharomyces cerevisiae* cells as the vaccine platform to develop a novel AD vaccine. The epitope was inserted between HA and c-Myc tags with a GSG linker, which enabled all the A β ₁₋₁₅ antigens to be presented on the surface of the recombinant *Saccharomyces cerevisiae* yeast (Figure 1a).

To further test the exhibition of 5 \times A β ₁₋₁₅ epitope on the surface, the yeast cells were incubated with anti-c-Myc antibody, then incubated with secondary antibody labelled with FITC, and detected by flow cytometer and confocal microscope, respectively. More than 90% Y-5A15 yeast cells showed positive signal in comparison to EBY100 alone (Figure 1b). Moreover, the confocal results confirmed that 5 \times A β ₁₋₁₅ peptides were displayed on the surface of the yeast cells, while no green fluorescence was detected on the EBY100 cell control (Figure 1c).

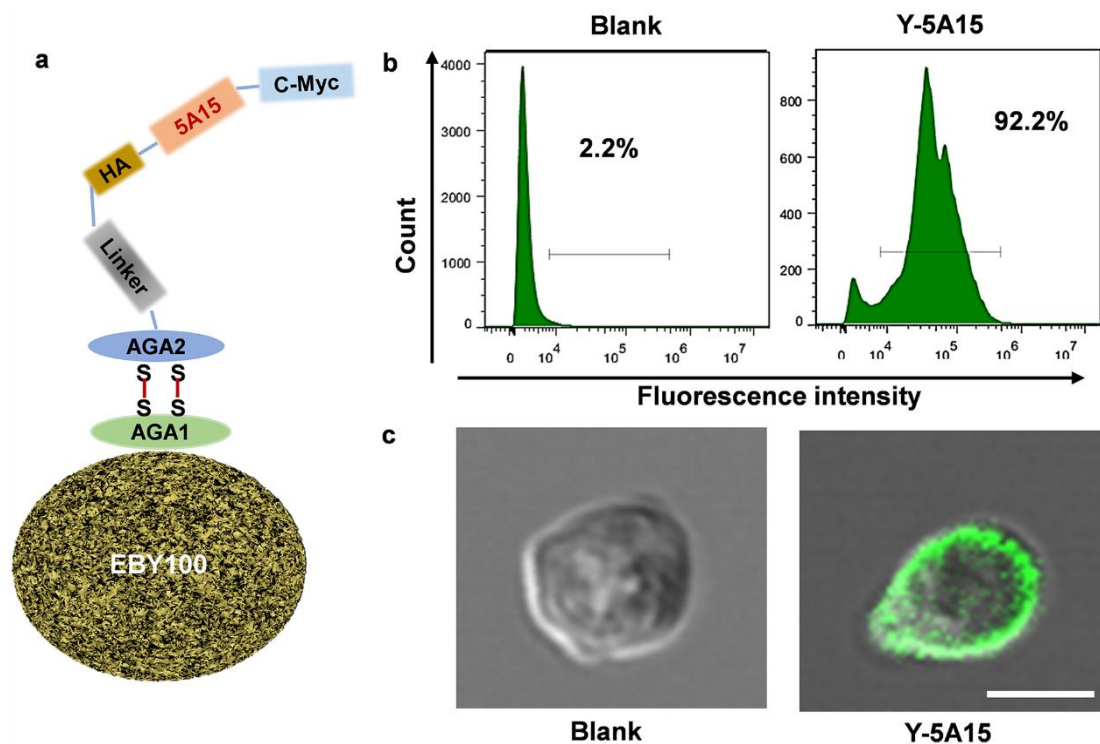


Figure 1. The construction and characterization of the A β 1–15 epitope on the EB100 yeast cell wall surface. (a) Schematic illustration of the construction of yeast-based vaccine. The epitope antigen with c-myc were displayed on the surface of cell wall by AGA2 interaction with AGA1. (b) The 5 \times A β 1–15 epitopes expressed on the surface the EB100 yeast cells were testified by flow cytometry using anti-c-Myc antibody and FITC-labeled secondary antibody. EB100 yeast cells were used as a negative control. (c) The 5 \times A β 1–15 epitopes in (b) were determined by confocal microscopy. Bar indicates 2 μ m.

3.2. Y-5A15 Vaccine Effectively Elicits High-Titer Antibodies against A β 42 in AD Mice

APP/PS1 mice were immunized subcutaneously with 6×10^7 Y-5A15 yeast cells for three times in the absence of adjuvant, and the serum antibody titer was detected by ELISA (Figure 2a). The results demonstrated that the Y-5A15 vaccine but not yeast vehicle (YEVC) induced a robust antibody response in mice (Figure 2b). The antibody titers increased with the immunization times and reached a plateau after the third vaccination (Figure 2b). Moreover, the antibody induced by YEVC had high affinity for A β monomer, oligomer and fibrillar (Figure 2d). The isotypes of the antibodies in response to A β 42 vaccine were detected by ELISA. Y-5A15 preferentially induced IgG1 antibody isotype (Figure 2c), indicating that predominant Th2 immune response was involved in Y-5A15 immunization.

To further detect the immune response, we performed IHC using antibody 6E10, the sera from Y-5A15 vaccine, as well as sera from YEVC-treated mice. The results showed that 6E10 and the sera induced by Y-5A15 vaccine bound to A β plaques in the brains of APP/PS1 mice, whereas no positive signal was observed with the addition of the sera from YEVC-treated mice, indicating that the induced antibodies recognized A β plaques (Figure 2e).

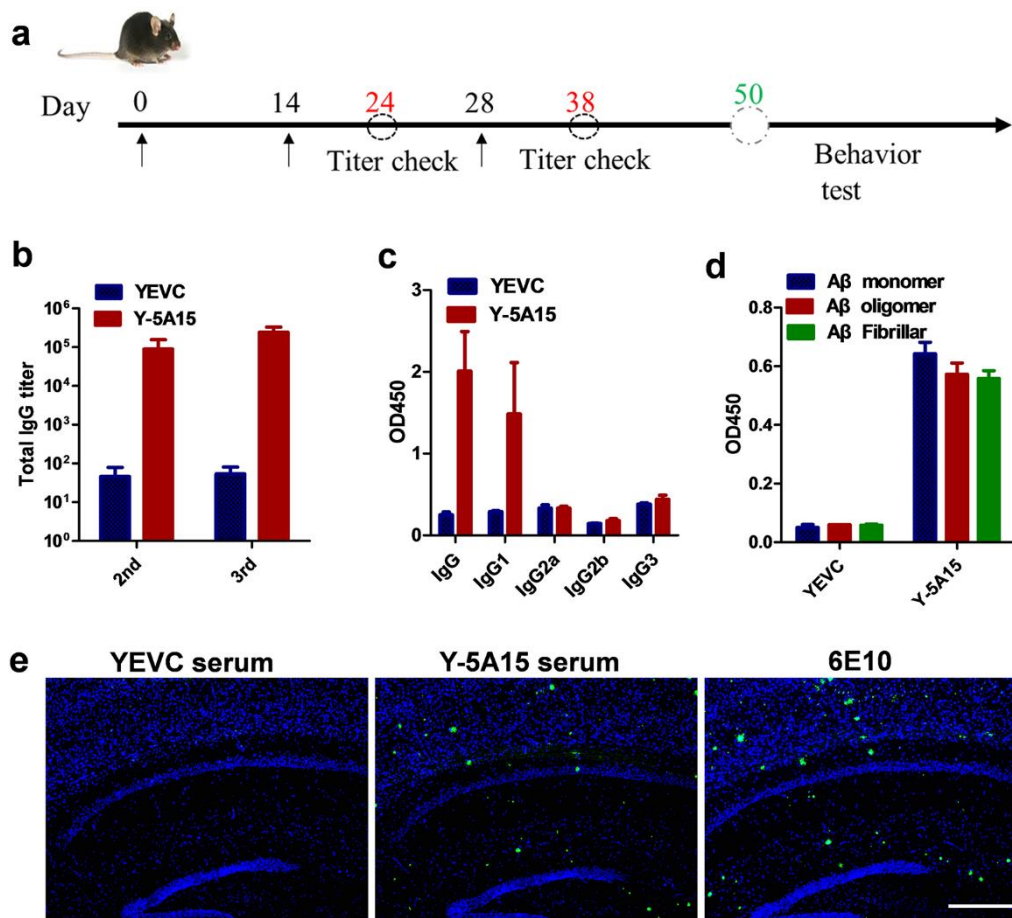


Figure 2. The anti-A β response of plasma antibody induced by Y-5A15 vaccine. (a) Schematic diagram of vaccine immunization for APP/PS1 mice ($n = 6$). (b) A β_{42} antibody levels induced by Y-5A15 vaccine. (c) The subtypes of vaccine-induced antibodies against A β_{42} . (d) The binding of antibodies induced by Y-5A15 vaccine to different A β isoforms was detected by ELISA. (e) Mice AD brain sections were stained using serum from Y-5A15-vaccinated APP/PS1 mice. Brain tissue was detected via IHC using serum from YEVC (1:200)- or Y-5A15 (1:200)-treated mice. Scale bar is 500 μm .

3.3. Y-5A15 Vaccination Attenuates Cognitive Impairment in APP/PS1 Mice

To evaluate the effect of Y-5A15 immunization on the cognition of APP/PS1 mice, we conducted behavioral tests, including spontaneous Y-maze, NOR and MWM tests. Compared with the YEVC-treated mice, Y-5A15-immunized mice spent more time in the new arm ($p < 0.05$) during the Y-maze test, indicating that Y-5A15 improved short-term memory in APP/PS1 mice (Figure 3a). During the probe trial of NOR test, the exploration times of mice treated with Y-5A15 for the novel object were significantly increased compared with the familiar object ($p < 0.05$), while the AD control and YEVC-treated mice exhibited similar exploration times on both novel and familiar objects (Figure 3b).

The MWM test was performed to detect the effects of Y-5A15 immunization on the spatial memory and learning ability of APP/PS1 mice. During the training phase of the test, the mice were given 1 min to search for the hidden platform under surface for 5 days. Compared with the AD control and YEVC-treated APP/PS1 mice, mice treated with Y-5A15 readily found the location of the hidden platform after 3 days of training ($p < 0.05$) (Figure 3c). After the last training, the mice were put in the maze to find the location of the removed platform for 1 min. Y-5A15-treated mice exhibited spatially oriented swimming behavior and shorter escape latencies (Figure 3d) and increased number of target crossings (Figure 3f), and they spent more time in the target quadrant (Figure 3e), indicating that Y-5A15 substantially improved the spatial memory and learning ability of APP/PS1 transgenic mice.

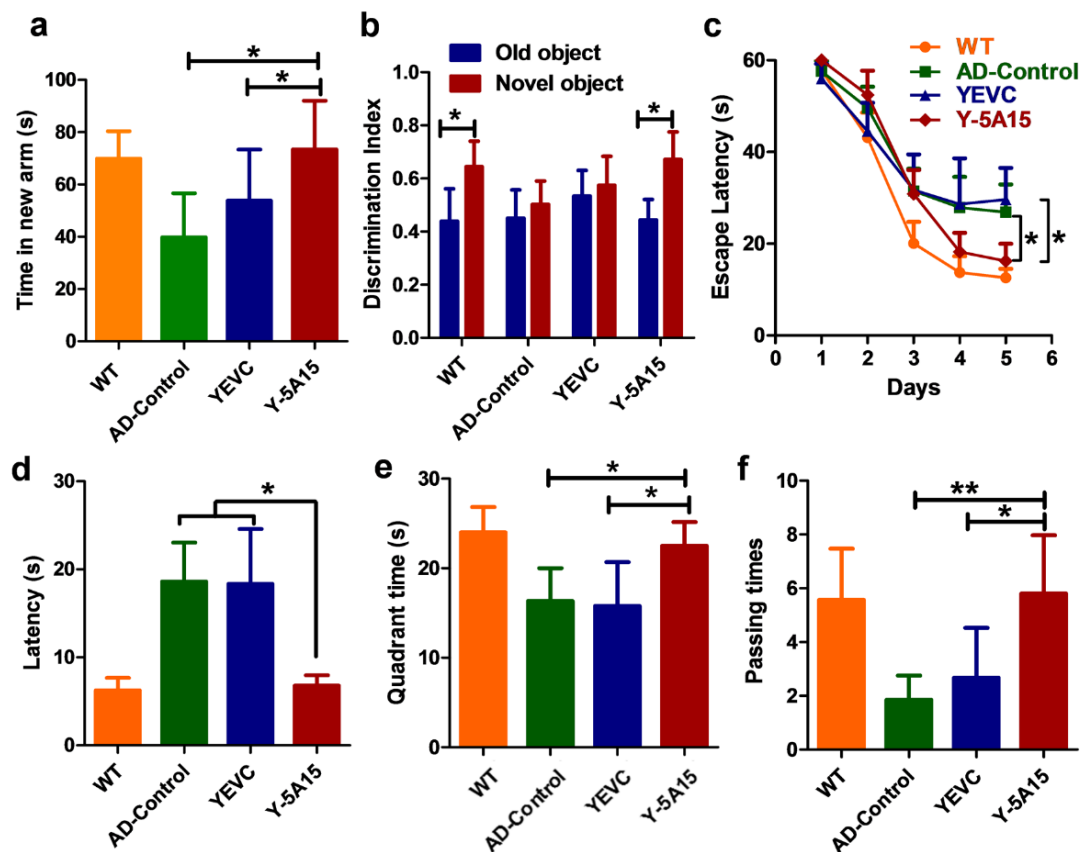


Figure 3. Y-5A15 vaccination improved cognitive capacity in APP/PS1 transgenic mice. (a) In the Y-maze, the time spent by mice in the new arm. (b) Discrimination index of AD mice tested by novel object recognition (NOR). (c) The escape latency in the acquisition period of the Morris water maze (MWM). (d) The escape latency in the probe trial of the MWM without the platform. (e) The target quadrant time in the MWM probe test. (f) The times of crossing the platform location in the MWM probe test. One-way ANOVA with LSD was used for statistical analysis. $n = 6$ mice per group, * $p < 0.05$, ** $p < 0.01$.

3.4. Y-5A15 Vaccination Reduces Cerebral A β Levels in AD Transgenic Mice

To study the effects of Y-5A15 vaccine on brain pathologies in AD mice, an initial evaluation of A β plaque burden was assessed in the cortex and hippocampus of mice (Figure 4a–c). Brain sections were immunolabelled with anti-human A β monoclonal antibody (mAb) 4G8 or fluorescently labelled with thioflavin-S (Thio-S) to assess diffused and mature/fibrillar A β plaque load, respectively. The results showed that 4G8⁺ A β plaque burden substantially reduced in the hippocampus of Y-5A15-treated mice but not in the YEVC-treated and AD control mice (Figure 4a). Moreover, in the brains of mice immunized with Y-5A15, the number of Thio-S⁺ A β plaque deposition also significantly relieved (Figure 4a). Quantitative analysis of A β plaque load on serial brain slices covering the hippocampus and cortex showed that compared with the AD control groups, Y-5A15-treated mice showed remarkable reduction in the levels of 4G8⁺ and Thio-S⁺ plaque by 53% and 60%, respectively ($p < 0.01$) (Figure 4b,c), indicating that Y-5A15 vaccination conspicuously alleviated the A β plaque load in the brain of APP/PS1 mice.

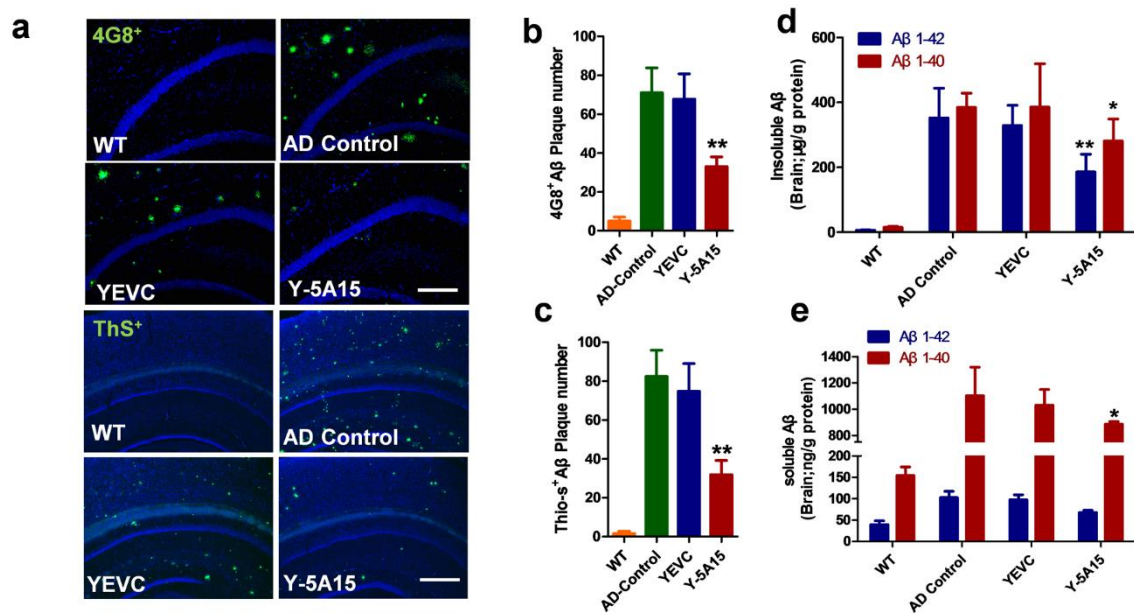


Figure 4. Y-5A15 immunization decreased cerebral amyloid- β ($A\beta$) peptide levels in the brains of APP/PS1 transgenic mice. (a) Representative microscopic images of brain sections from different groups. Sections were stained with the anti-human $A\beta$ antibody 4G8 (Green) and thioflavin S (ThS), counterstained with DAPI (blue) to detect nuclei. The number of 4G8-positive (b) and ThS-positive plaques (c) were quantified in the hippocampus (Hip) and cortex (Ctx) by IpWin5 software. (d) ELISA analyses of insoluble human $A\beta_{40}$ and $A\beta_{42}$ in the brains. (e) ELISA analyses of soluble human $A\beta_{40}$ and $A\beta_{42}$ in the brains. Compared with AD control, * $p < 0.05$, ** $p < 0.01$, Student's t -test, $n = 6$ mice per group. Scale bar is 200 μm .

The levels of insoluble $A\beta_{40}$ and $A\beta_{42}$ in the brains of mice immunized with Y-5A15 significantly decreased by 27% and 47%, respectively (Figure 4d,e). The Y-5A15 vaccine effectively relieved the level of $A\beta_{40}$ by 21% in soluble brain extracts (Figure 4e, Red bars), but has no significant effect on the level of soluble $A\beta_{42}$ (Figure 4e, Blue bars). Taken together, these results demonstrated that Y-5A15 vaccination significantly reduced the amount of plaque deposition and levels of $A\beta_{40}$ and $A\beta_{42}$ in the brain of APP/PS1 mice.

3.5. Y-5A15 Vaccination Suppresses Astrogliosis and Microgliosis in the Brains of AD Mice

In AD, microglia and astrocytes accumulate at $A\beta$ plaque lesion sites and exhibit increased reactivity and cytotoxicity. Overactivation of glial cells may be involved in vascular disease in mixed dementia and even in “pure” AD pathology [28]. To address whether vaccine treatment was effective for astrogliosis and microgliosis in the brains of APP/PS1 transgenic mice, we stained astrocytes and microglia with antibodies against Iba-1 and GFAP, respectively. The results showed that Y-5A15 vaccination reduced microgliosis especially in the cortical and hippocampal regions (Figure 5).

Quantitative immunohistochemical analyses of Iba1⁺ and GFAP⁺ cells' total area were performed in the cortex and hippocampal regions from each experimental group. Y-5A15 strongly reduced mean cortical and hippocampal Iba1⁺ cell area by 54% and 52%, respectively (Figure 5c). Moreover, Y-5A15 treatment remarkably reduced mean cortical and hippocampal GFAP⁺ cell area by 53% and 46%, respectively (Figure 5d). These results suggested that Y-5A15 treatment significantly suppressed astrogliosis and microgliosis in AD mouse brain, which may also benefit for vascular cognitive impairment acting as a disease-modifying molecule [29].

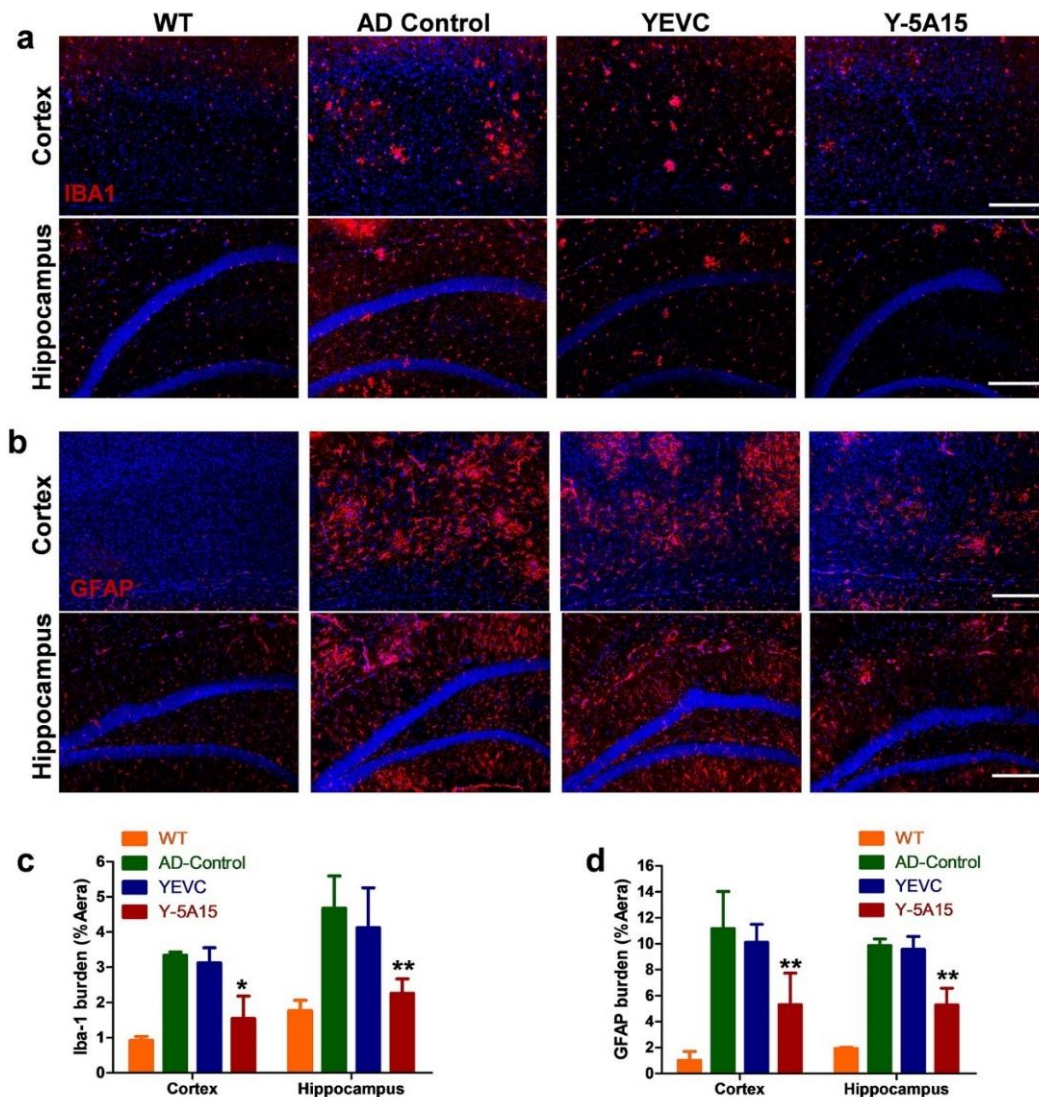


Figure 5. Y-5A15 vaccination decreased activated microglia and astrocytes in the hippocampus and cortex of APP/PS1 transgenic mice. (a) Representative fluorescence micrographs in the cortex and hippocampus of brain slices detected by staining Iba-1, and then the stained microglia were quantified using IpWin5 software (c). (b) Astrocytes in the cortex and hippocampus of brain slices were determined by staining GFAP, and then the stained astrocytes were quantified using IpWin5 software (d). Compared with AD control, * $p < 0.05$, ** $p < 0.01$, Student's t -test, $n = 6$ mice per group. Scale bar is 200 μm .

3.6. Active Immunotherapy by Y-5A15 Yeast Vaccine Rescues Synaptic Deficits in APP/PS1 Mice

The $A\beta$ accumulation and accompanying neuronal loss have been corroborated in the previous studies [30,31]. To assess whether the reduction of $A\beta$ accumulation can attenuate synaptic deficits, we used anti-synaptophysin antibody to detect the effect of Y-5A15 yeast vaccine on the synapses. AD mice vaccinated with Y-5A15 showed significantly higher synaptophysin densities in the cortex and hippocampal regions compared with control groups (Figure 6), indicating that Y-5A15 yeast immunization rescued $A\beta$ -induced synaptic deficits in APP/PS1 mice.

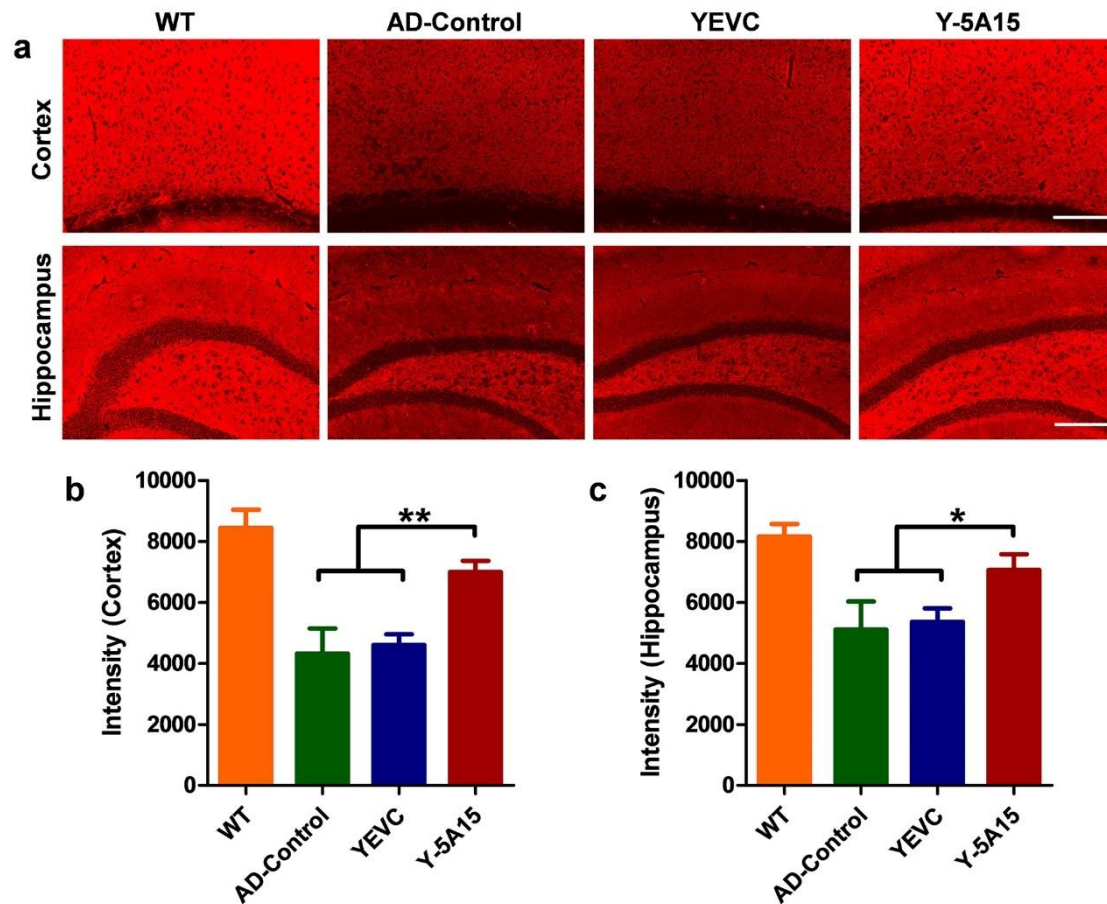


Figure 6. Active immunotherapy using Y-5A15 vaccine rescued synaptic deficits in APP/PS1 transgenic mice. (a) Presynapses in brains of mice were detected by IHC with anti-synaptophysin antibody in various immunized groups. Synaptophysin in the cortex and the hippocampal regions (b,c) was quantified using IPwin5 Image-Pro Plus software, respectively, and results are shown in arbitrary units (AU). * $p < 0.05$, ** $p < 0.01$. Scale bar is 200 μm .

4. Discussion

We here designed and prepared a *Saccharomyces cerevisiae*-based AD vaccine, Y-5A15, and provided strong evidences that Y-5A15 yeast vaccine could serve as effective antigen carrier and adjuvant to enhance the immunogenicity of A β 1–15, and induced rapid antibody production, exerting favorable effects on cognition and neuropathology in the APP/PS1 mice.

In order to improve immunogenicity of the short A β 1–15 peptide, we constructed a five-valent foldable A β 1–15 in the design of Y-5A15 yeast vaccine, with a GSG small linker separating each peptide sequence ($5 \times \text{A}\beta$ 15). Consistent with the previous report that *S. cerevisiae* yeast expressed high copies of the protein scaffold-Aga2 fusions [23], the $5 \times \text{A}\beta$ 1–15 peptides were densely displayed on the yeast cell wall and over 90% Y-5A15 yeast cells expressed antigen. All AD mice immunized with Y-5A15 yeast vaccine developed sufficient A β antibody titers. Our further results demonstrated that the induced A β antibody had a high affinity to A β monomer, oligomers and fibers, indicating that Y-5A15 vaccine may reduce insoluble A β or A β deposits as well as soluble forms of A β , including the neurotoxic oligomers which impair synaptic and cognitive function [32]. Importantly, the predominant antibody induced by Y-5A15 vaccine was IgG1 isotype, indicating that the immune response to the vaccine was mainly involved in the Th2 phenotype and that yeast-derived carrier may be a safe vaccine platform.

High A β antibody titers induced by Y-5A15 vaccine attenuated cognitive impairment in APP/PS1 mice. NOR, Y-maze and Morris water maze tests were performed to evaluate the efficiency of Y-5A15 vaccination in improving cognitive function in APP/PS1. Y-5A15-treated mice demonstrated a

significant improvement in novel object exploration, short-term memory and spatial memory. Fibrillar A β plaques have been demonstrated to correlate with microglycosis and astrocytosis in AD transgenic mouse models and patients [33–35]. In the study, the A β plaques were attenuated in the immunized APP/PS1 mice, which was consistent with the decrease of insoluble A β extracted from the brain. These results may further induce fewer Iba-1-immunopositive microglia and GFAP-immunopositive astrocytes. Moreover, Y-5A15-vaccinated APP/PS1 mice had higher synaptic density, which may contribute to their superior cognitive performance compared to the control AD mice. Like other vaccines using yeast as a carrier, Y-5A15 yeast vaccine was characterized by easy preparation, good safety, and low cost [36], suggesting that Y-5A15 held promising potential for AD treatment. However, before the translation of Y-5A15 into clinical application, its acute and long-term toxicity, long term stability, pharmacokinetics, and the duration of the induced antibody in peripheral blood should be detected.

5. Conclusions

In conclusion, our study indicated that the yeast-based Y-5A15 vaccine exerted favorable effects on cognition and neuropathology in the APP/PS1 mice by inducing high titers of antibodies against A β , decreasing A β burden, suppressing microgliosis and astrogliosis in mouse brains, and increasing synaptophysin levels. These findings suggest that Y-5A15 may be a safe and effective vaccine for the treatment of AD.

Author Contributions: Conceptualization, R.-t.L.; Formal analysis, D.-q.L. and L.Z.; Funding acquisition, R.-t.L.; Investigation, D.-q.L., M.J., X.-y.S., X.-g.L. and L.Z.; Methodology, R.-t.L.; Resources, R.-t.L.; Supervision, R.-t.L.; Visualization, R.-t.L. and S.L.; Writing—original draft, D.-q.L.; Writing—review & editing, R.-t.L., S.L. and Y.-r.H. All authors have read and agreed to the published version of the manuscript.

Funding: This work was supported by grants from the National Natural Science Foundation of China [31401158,81972444].

Conflicts of Interest: There are no conflict to declare.

References

1. Selkoe, D.J. The molecular pathology of Alzheimer's disease. *Neuron* **1991**, *6*, 487–498. [[CrossRef](#)]
2. Selkoe, D.J. Alzheimer's disease: A central role for amyloid. *J. Neuropathol. Exp. Neurol.* **1994**, *53*, 438–447. [[CrossRef](#)] [[PubMed](#)]
3. Cline, E.N.; Bicca, M.A.; Viola, K.L.; Klein, W.L. The amyloid-beta oligomer hypothesis: Beginning of the third decade. *J. Alzheimer's Dis. JAD* **2018**, *64*, S567–S610. [[CrossRef](#)] [[PubMed](#)]
4. Cleary, J.P.; Walsh, D.M.; Hofmeister, J.J.; Shankar, G.M.; Kuskowski, M.A.; Selkoe, D.J.; Ashe, K.H. Natural oligomers of the amyloid-beta protein specifically disrupt cognitive function. *Nat. Neurosci.* **2005**, *8*, 79–84. [[CrossRef](#)] [[PubMed](#)]
5. Klein, W.L.; Stine, W.B., Jr.; Teplow, D.B. Small assemblies of unmodified amyloid beta-protein are the proximate neurotoxin in Alzheimer's disease. *Neurobiol. Aging* **2004**, *25*, 569–580. [[CrossRef](#)]
6. Shankar, G.M.; Li, S.M.; Mehta, T.H.; Garcia-Munoz, A.; Shepardson, N.E.; Smith, I.; Brett, F.M.; Farrell, M.A.; Rowan, M.J.; Lemere, C.A.; et al. Amyloid-beta protein dimers isolated directly from Alzheimer's brains impair synaptic plasticity and memory. *Nat. Med.* **2008**, *14*, 837–842. [[CrossRef](#)]
7. Selkoe, D.J. Light at the End of the Amyloid Tunnel. *Biochemistry* **2018**, *57*, 5921–5922. [[CrossRef](#)]
8. Ferrer, I.; Rovira, M.B.; Guerra, M.L.S.; Rey, M.J.; Costa-Jussa, F. Neuropathology and pathogenesis of encephalitis following amyloid-beta immunization in Alzheimer's disease. *Brain Pathol.* **2004**, *14*, 11–20. [[CrossRef](#)]
9. Nicoll, J.A.R.; Wilkinson, D.; Holmes, C.; Steart, P.; Markham, H.; Weller, R.O. Neuropathology of human Alzheimer disease after immunization with amyloid-beta peptide: A case report. *Nat. Med.* **2003**, *9*, 448–452. [[CrossRef](#)]
10. Bachmann, M.F.; Jennings, G.T.; Vogel, M. A vaccine against Alzheimer's disease: Anything left but faith? *Expert Opin. Biol. Ther.* **2019**, *19*, 73–78. [[CrossRef](#)]

11. Holmes, C.; Boche, D.; Wilkinson, D.; Yadegarfar, G.; Hopkins, V.; Bayer, A.; Jones, R.W.; Bullock, R.; Love, S.; Neal, J.W.; et al. Long-term effects of A beta(42) immunisation in Alzheimer's disease: Follow-up of a randomised, placebo-controlled phase I trial. *Lancet* **2008**, *372*, 216–223. [[CrossRef](#)]
12. Gilman, S.; Koller, M.; Black, R.S.; Jenkins, L.; Griffith, S.G.; Fox, N.C.; Eisner, L.; Kirby, L.; Rovira, M.B.; Forette, F.; et al. Clinical effects of Abeta immunization (AN1792) in patients with AD in an interrupted trial. *Neurology* **2005**, *64*, 1553–1562. [[CrossRef](#)] [[PubMed](#)]
13. Sevigny, J.; Chiao, P.; Bussiere, T.; Weinreb, P.H.; Williams, L.; Maier, M.; Dunstan, R.; Salloway, S.; Chen, T.; Ling, Y.; et al. The antibody aducanumab reduces Abeta plaques in Alzheimer's disease. *Nature* **2016**, *537*, 50–56. [[CrossRef](#)]
14. von Hehn, C.; von Rosenstiel, P.; Tian, Y.; Wu, S.; Chen, T.L.; Skordos, L.; Harrison, K.; Prada, C.; Chalkias, S.; Rajagovindan, R.; et al. Baseline characteristics from ENGAGE and EMERGE: Two phase 3 studies to evaluate aducanumab in patients with early Alzheimer's disease (P4.1-001). *Neurology* **2019**, *92*. Available online: https://n.neurology.org/content/92/15_Supplement/P4.1-001 (accessed on 26 May 2020).
15. Winblad, B.; Andreasen, N.; Minthon, L.; Floesser, A.; Imbert, G.; Dumortier, T.; Maguire, R.P.; Blennow, K.; Lundmark, J.; Staufenbiel, M.; et al. Safety, tolerability, and antibody response of active Abeta immunotherapy with CAD106 in patients with Alzheimer's disease: Randomised, double-blind, placebo-controlled, first-in-human study. *Lancet Neurol.* **2012**, *11*, 597–604. [[CrossRef](#)]
16. Agadjanyan, M.G.; Ghochikyan, A.; Petrushina, I.; Vasilevko, V.; Movsesyan, N.; Mkrtichyan, M.; Saing, T.; Cribbs, D.H. Prototype Alzheimer's disease vaccine using the immunodominant B cell epitope from beta-amyloid and promiscuous T cell epitope pan HLA DR-binding peptide. *J. Immunol.* **2005**, *174*, 1580–1586. [[CrossRef](#)]
17. Arai, H.; Suzuki, H.; Yoshiyama, T. Vanutide cridificar and the QS-21 Adjuvant in Japanese subjects with mild to moderate Alzheimer's Disease: Results from two phase 2 studies. *Curr. Alzheimer Res.* **2015**, *12*, 242–254. [[CrossRef](#)] [[PubMed](#)]
18. Geylis, V.; Kourilov, V.; Meiner, Z.; Nennesmo, I.; Bogdanovic, N.; Steinitz, M. Human monoclonal antibodies against amyloid-beta from healthy adults. *Neurobiol. Aging* **2005**, *26*, 597–606. [[CrossRef](#)]
19. Wadle, A.; Held, G.; Neumann, F.; Kleber, S.; Wuellner, B.; Asemissen, A.M.; Kubuschok, B.; Scheibenbogen, C.; Breinig, T.; Meyerhans, A.; et al. Cross-presentation of HLA class I epitopes from influenza matrix protein produced in *Saccharomyces cerevisiae*. *Vaccine* **2006**, *24*, 6272–6281. [[CrossRef](#)]
20. Howland, S.W.; Wittrup, K.D. Antigen release kinetics in the phagosome are critical to cross-presentation efficiency. *J. Immunol.* **2008**, *180*, 1576–1583. [[CrossRef](#)]
21. Chao, G.; Lau, W.L.; Hackel, B.J.; Sazinsky, S.L.; Lippow, S.M.; Wittrup, K.D. Isolating and engineering human antibodies using yeast surface display. *Nat. Protoc.* **2006**, *1*, 755. [[CrossRef](#)]
22. Zhou, W.W.; Lu, S.; Su, Y.J.; Xue, D.; Yu, X.L.; Wang, S.W.; Zhang, H.; Xu, P.X.; Xie, X.X.; Liu, R.T. Decreasing oxidative stress and neuroinflammation with a multifunctional peptide rescues memory deficits in mice with Alzheimer disease. *Free Radic. Biol. Med.* **2014**, *74*, 50–63. [[CrossRef](#)] [[PubMed](#)]
23. Oakley, H.; Cole, S.L.; Logan, S.; Maus, E.; Shao, P.; Craft, J.; Guillozet-Bongaarts, A.; Ohno, M.; Disterhoft, J.; Van Eldik, L.; et al. Intraneuronal beta-amyloid aggregates, neurodegeneration, and neuron loss in transgenic mice with five familial Alzheimer's disease mutations: Potential factors in amyloid plaque formation. *J. Neurosci. Off. J. Soc. Neurosci.* **2006**, *26*, 10129–10140. [[CrossRef](#)] [[PubMed](#)]
24. Pozueta, J.; Lefort, R.; Shelanski, M.L. Synaptic changes in Alzheimer's disease and its models. *Neuroscience* **2013**, *251*, 51–65. [[CrossRef](#)] [[PubMed](#)]
25. Anand, R.; Gill, K.D.; Mahdi, A.A. Therapeutics of Alzheimer's disease: Past, present and future. *Neuropharmacology* **2014**, *76*, 27–50. [[CrossRef](#)]
26. Logovinsky, V.; Satlin, A.; Lai, R.; Swanson, C.; Kaplow, J.; Osswald, G.; Basun, H.; Lannfelt, L. Safety and tolerability of BAN2401—a clinical study in Alzheimer's disease with a protofibril selective A beta antibody. *Alzheimers Res. Ther.* **2016**, *8*. [[CrossRef](#)]
27. Loureiro, J.C.; Pais, M.V.; Stella, F.; Radanovic, M.; Teixeira, A.L.; Forlenza, O.V.; de Souza, L.C. Passive anti-amyloid immunotherapy for Alzheimer's disease. *Curr. Opin. Psychiatry* **2020**, *33*, 284–291. [[CrossRef](#)]
28. Vellas, B.; Black, R.; Thal, L.J.; Fox, N.C.; Daniels, M.; McLennan, G.; Tompkins, C.; Leibman, C.; Pomfret, M.; Grundman, M.; et al. Long-term follow-up of patients immunized with AN1792: Reduced functional decline in antibody responders. *Curr. Alzheimer Res.* **2009**, *6*, 144–151. [[CrossRef](#)]

29. Lobello, K.; Ryan, J.M.; Liu, E.; Rippon, G.; Black, R. Targeting Beta amyloid: A clinical review of immunotherapeutic approaches in Alzheimer's disease. *Int. J. Alzheimer's Dis.* **2012**, *2012*, 628070. [[CrossRef](#)]
30. Petrushina, I.; Davtyan, H.; Hovakimyan, A.; Davtyan, A.; Passos, G.F.; Cribbs, D.H.; Ghochikyan, A.; Agadjanyan, M.G. Comparison of efficacy of preventive and therapeutic vaccines targeting the N terminus of beta-amyloid in an animal model of Alzheimer's disease. *Mol. Ther. J. Am. Soc. Gene Ther.* **2017**, *25*, 153–164. [[CrossRef](#)]
31. Lambert, M.P.; Barlow, A.K.; Chromy, B.A.; Edwards, C.; Freed, R.; Liosatos, M.; Morgan, T.E.; Rozovsky, I.; Trommer, B.; Viola, K.L.; et al. Diffusible, nonfibrillar ligands derived from Abeta1-42 are potent central nervous system neurotoxins. *Proc. Natl. Acad. Sci. USA* **1998**, *95*, 6448–6453. [[CrossRef](#)]
32. Mandler, M.; Santic, R.; Gruber, P.; Cinar, Y.; Pichler, D.; Funke, S.A.; Willbold, D.; Schneeberger, A.; Schmidt, W.; Mattner, F. Tailoring the antibody response to aggregated Ass using novel Alzheimer-vaccines. *PLoS ONE* **2015**, *10*, e0115237. [[CrossRef](#)] [[PubMed](#)]
33. Frautschy, S.A.; Yang, F.; Irrizarry, M.; Hyman, B.; Saito, T.C.; Hsiao, K.; Cole, G.M. Microglial response to amyloid plaques in APPsw transgenic mice. *Am. J. Pathol.* **1998**, *152*, 307–317. [[PubMed](#)]
34. Gordon, M.N.; Holcomb, L.A.; Jantzen, P.T.; DiCarlo, G.; Wilcock, D.; Boyett, K.W.; Connor, K.; Melachrinou, J.; O'Callaghan, J.P.; Morgan, D. Time course of the development of Alzheimer-like pathology in the doubly transgenic PS1+APP mouse. *Exp. Neurol.* **2002**, *173*, 183–195. [[CrossRef](#)] [[PubMed](#)]
35. Koronyo, Y.; Salumbides, B.C.; Sheyn, J.; Pelissier, L.; Li, S.; Ljubimov, V.; Moyseyev, M.; Daley, D.; Fuchs, D.T.; Pham, M.; et al. Therapeutic effects of glatiramer acetate and grafted CD115(+) monocytes in a mouse model of Alzheimer's disease. *Brain J. Neurol.* **2015**, *138*, 2399–2422. [[CrossRef](#)] [[PubMed](#)]
36. Ardiani, A.; Higgins, J.P.; Hodge, J.W. Vaccines based on whole recombinant *Saccharomyces cerevisiae* cells. *FEMS Yeast Res.* **2010**, *10*, 1060–1069. [[CrossRef](#)]



© 2020 by the authors. Licensee MDPI, Basel, Switzerland. This article is an open access article distributed under the terms and conditions of the Creative Commons Attribution (CC BY) license (<http://creativecommons.org/licenses/by/4.0/>).